Nuclear Instruments and M..nods in Physics Research A279 (1989) 603–610
North-Holland, Amsterdam

THE STANDARDIZATION OF PLUTONIUM-241 AND NICKEL-63

B.M. COURSEY and L.L. LUCAS

*Center for Radiation Research, National Institute of Standards and Technology *, Gaithersburg, Maryland 20899, USA*

A. GRAU MALONDA and E. GARCIA-TORAÑO

Centro de Investigaciones Energeticas Medioambientales y Technologicas, Madrid 28040, Spain

Received 27 February 1989

Solutions of the low-energy beta-particle emitters ^{241}Pu and ^{63}Ni have been standardized using the method of $4\pi\beta$ liquid scintillation (LS) efficiency tracing with ^{3}H. The ^{241}Pu has also been standardized by the method of $4\pi\alpha$(LS)–γ coincidence and anticoincidence counting of the ^{241}Am daughter to follow its ingrowth in a separated sample. The ^{63}Ni solution was previously standardized at NIST by calorimetry. The uncertainties in the radioactivity concentrations obtained using these methods are discussed.

1. Introduction

The low-energy beta emitters ^{241}Pu (20.82 keV) and ^{63}Ni (65.88 keV) [1] are difficult to standardize for activity because of the short range of the beta particles. Such standards are needed for the assay of ^{241}Pu in mixed Pu isotopes and for the assay of ^{63}Ni in power reactor waste samples. Table 1 lists the pertinent nuclear decay data for these two radionuclides. Table 2 gives a selected list of methods which have been used to standardize the two radionuclides. There are, of course, advantages and disadvantages associated with each method. Due to the relatively long half-lives, mass spectrometric methods will give good results for MBq activity samples. Mass spectrometers, however, are not available in all laboratories which have requirements for assaying these nuclides.

Calorimetry has been used for ^{63}Ni [2], but the samples were 50 GBq each. Samples of ^{241}Pu of comparable power level would require a factor of 3 more activity (corresponding to about 4 Ci). An additional drawback to calorimetric assays of ^{241}Pu is that large corrections are necessary to correct the observed power for the other Pu isotopes and the ^{241}Am daughter, all of which are alpha-particle emitters.

Of the counting techniques, the best known is the $4\pi\beta$–γ coincidence efficiency-tracing method [3,4]. In this method a β–γ emitter is first standardized using the conventional $4\pi\beta$–γ coincidence method. The beta-particle detector is usually a pressurized proportional counter, but may also be a liquid scintillator, while the gamma-ray detector usually consists of one or two NaI(Tl) crystals. Mixed radionuclide samples of the β–γ emitter and the pure β emitter are then measured, and the efficiency of the latter is "traced" with that of the standard β–γ emitting nuclide. The method works best when the two nuclides have similar β-spectrum shapes in the low-energy region [5]. Two Canadian (AECL [6], NRC [7]) and one Austrialian (AAEC [8]) national standards laboratories have used this method to standardize ^{63}Ni. All three groups used ^{60}Co as the tracer nuclide, thin-film sources, and proportional counters as the β detectors. Lowenthal et al. [8] were able to obtain β-particle detection efficiencies approaching 86% for ^{63}Ni, which are comparable to those obtained with two-phototube liquid-scintillation (LS) systems. We have

Table 1
Selected nuclear data for ^{241}Pu and ^{63}Ni

	^{241}Pu	^{63}Ni
Half-life [yr]	14.35±0.10	100.07±2.00 [2]
$E_{\beta max}$ [keV] (ref. [1])	20.82±0.20	65.88±0.15 [1]
$E_{\beta ave}$ [keV] (ref. [1])	5.23±0.05	17.13±0.04 [1]
Atomic mass [g]	241.0568	62.9297
Specific activity [Bq/g]	3.824×10^{12}	2.113×10^{12}
Specific power [μW/TBq]	0.838	2.744
Alpha-particle branch	$(2.46\pm0.01)\times10^{-5}$	none

* Formerly National Bureau of Standards.

Table 2
Methods fo standardizing ^{241}Pu and ^{63}Ni

	Method	Ref.
^{241}Pu	Mass spectrometry	[24]
	Daughter ingrowth	[26]
	Sum-to-coincidence LS counting	[9]
	Singles-to-coincidence LS counting	[10]
^{63}Ni	Calorimetry	[2]
	Efficiency tracing with ^{60}Co	[6–8]
	Discriminator-extrapolation LS counting	[25]
	4πβ(LS) efficiency tracing with ^{14}C	[23]
	Triple-to-double-coincidence LS counting	[12]

found no record of this method having been applied to ^{241}Pu β-particle measurements.

Several LS techniques have been used for direct activity measurements of low-energy β emitters since the early work of Horrocks and Studier [9]. One of the radionuclides they considered was ^{241}Pu, and this method was extended by Denecke et al. [10] for ^{241}Pu to give the relationship between the singles (individual phototube) and coincidence counting rates for two-phototube counting systems. The disadvantage to this approach is that one must accurately measure the singles counting rate, which includes both a significant background due to thermionic emission (dark current) and a contribution due to after pulsing [11].

More recently Pochwalski et al. [12] have used a triple phototube LS counter for ^{63}Ni. In this case the triple-to-double-coincidence ratio (TDCR) is extrapolated to unit efficiency and the activity of the sample is obtained without recourse to other standards, and without using the singles counting rates.

In the present work we apply the method of 4πβ(LS)-efficiency tracing with ^{3}H [13–15]. The theory of this method has been described in some detail in a recent paper on the standardization of ^{14}C [15]. The coincidence counting efficiency, ϵ_c, for a pure β emitter in a two-phototube coincidence counting system is given by

$$\epsilon_c = \left\{ \int_0^{E_{\beta max}} P(Z, E) \times [1 - \exp(-E\eta Q(E) W(E))]^2 \, dE \right\} \times \left\{ \int_0^{E_{\beta max}} P(Z, E) \, dE \right\}^{-1}, \quad (1)$$

where $P(Z, E)\,dE$ is the Fermi distribution function, η is the figure of merit, photoelectrons per keV, $Q(E)$ is the ionization quenching function, and $W(E)$ is a wall-loss function, taken here as unity for these low-energy β particles.

A LS sample of ^{3}H-water of known activity, N_0, is measured and its beta-particle counting rate in the coincidence mode, N_β, is used to calculate the counting efficiency as $\epsilon_c = N_\beta / N_0$. Best estimates are then established for the η and $Q(E)$ terms in eq. (1) such that the integration for ^{3}H leads to the observed value for ϵ_c.

With the system calibrated in this manner, eq. (1) can be used to compute the counting efficiency for other pure-β emitters providing the β energy distributions are known. The method has been demonstrated for ^{14}C [15] and ^{99}Tc [14], which have maximum β energies of 156.5 and 293.5 keV, respectively. We were interested in seeing if the method could be applied also to the standardization of ^{241}Pu and ^{63}Ni, as these are the two low-energy pure-β emitters of greatest practical interest.

The ^{241}Pu measurements were made on a sample obtained from Oak Ridge National Laboratory (ORNL) shortly after a Pu separation was performed at ORNL on March 10, 1977. Since that time we have been following the ingrowth of the ^{241}Am ($T_{1/2}$ = 432.2 yr) by 4πα(LS)–γ coincidence and anticoincidence counting. We are thus able to compare the activity results from β counting of ^{241}Pu with those obtained indirectly by α counting of the ^{241}Am daughter.

The measurements on ^{63}Ni were carried out on NIST Standard Reference Material (SRM) 4226B, the same material previously standardized at NIST by calorimetry [2]. Due to its long half-life, and the high purity and stability of this material, it is possible to compare the present results with those from several other laboratories taken over a period of 18 years.

2. Experimental section

2.1. Materials

The ^{241}Pu (74 MBq) from ORNL was examined for radionuclidic impurities and all the emissions observed could be attributed to ^{241}Pu plus progeny. The ORNL material was diluted with 5M nitric acid. The diluted samples have been distributed as NIST SRM 4340.

The preparation of the ^{63}Ni used for SRM 4226B has been described by Barnes et al. [2]. The material was produced by a high-flux reactor irradiation at Savannah River of an ORNL-prepared, enriched ^{62}Ni target. Thus, the material does not contain the long-lived ^{59}Ni normally present along with ^{63}Ni as a reactor activation product. The only impurity noted in the 1969 certificate was 1.6 ppm of ^{110m}Ag (249 d half-life). The chemical form of the standard solution is 83 μg of Ni as $NiCl_2$ per gram of 1N hydrochloric acid.

The ^{3}H-water standard used was gravimetrically related to SRM 4927B [16].

The premixed scintillator used was * PCS (Amersham Corp.). For the ^{241}Pu samples it was necessary to add a chelating agent, di-ethylhexyl phosphoric acid HDEHP [17] (K&K Laboratories), to prevent loss of plutonium from the scintillator. The HDEHP concentration was 0.05M in the PCS solution.

Measurements of ^{241}Pu and ^{63}Ni in the commercial liquid-scintillation counter were made using 10 ml of scintillator in standard 2.7 cm o.d. screw-cap vials. The ^{241}Pu α–γ coincidence measurements were made using 3.5 ml of scintillator in glass hemispheres of 3.8 cm o.d.

2.2. Equipment

The efficiency-tracing measurements reported here were made using a Beckman model LS7800 counter operating at ambient temperature. Previously, measurements using these same materials and scintillators were made with a Packard model 3320 operated at 6 °C.

The $4\pi\alpha$(LS)–γ coincidence and anticoincidence measurements were made using the detector described by Lucas [18]. This system consists of a single RCA 8575 phototube for the LS alpha-particle detector and a 5 in. × 4 in. NaI(Tl) crystal with a 2 in. well as the gamma-ray detector. The hemispherical cell containing the scintillator is coupled with silicone grease to the face of the vertically mounted phototube and the NaI(Tl) well crystal is lowered over the cell-phototube from above.

2.3. Methods

The samples were prepared by gravimetrically depositing 20–70 mg of the aqueous sample into the vials containing scintillator. For the efficiency-tracing measurements three sets of vials were prepared: one each containing ^{3}H, ^{241}Pu, or ^{63}Ni. In each set, two samples were deaerated with argon gas to obtain the highest possible counting efficiency.

Each set of vials was monitored over a period of weeks to study the sample stability. For ^{241}Pu containing HDEHP the stability was excellent. It was possible to combine data taken over 17 days.

For the ^{3}H and ^{63}Ni, problems were observed which are related to the stability of the reverse micelles formed when water is dispersed in the organic scintillators. Previous measurements with PCS (containing of the order of 1% water) at 6 °C gave extremely reproducible counting efficiencies for ^{3}H, ^{241}Pu and ^{63}Ni over long periods.

At ambient temperature, however, the micelle structure appears to collapse with time (a film of finely dispersed water droplets can be seen) resulting in a decrease in ^{3}H-water counting efficiencies of about 0.16% per day. We usually use ^{3}H data only from the first few hours after sample preparation. With ^{63}Ni, losses were also observed in the count rates of about 0.1% per day and neither HDEHP nor additional Ni carrier could prevent this loss. The same problem has been observed with different radionuclides (^{55}Fe) and scintillators (Beckman Readysolv HP). A detailed study of this phenomenon would require measuring the temperature dependence of the distribution coefficient of the cation between the aqueous and organic phases. For the ^{241}Pu samples, the chelated cation appears to stay in the organic phase and the count rates are constant.

3. Results and discussion

3.1. Standardization of ^{241}Pu by ^{241}Am-daughter-ingrowth measurements

The half-lives of ^{241}Pu (14.35 ± 0.10 yr) [19] and ^{241}Am (432.2 ± 0.5 yr) [19] are now fairly well established. ^{241}Pu decays [19] partially by alpha-particle emission ($f_\alpha = (2.46 \pm 0.01) \times 10^{-5}$) but primary by beta-particle emission to ^{241}Am. ^{241}Am decays totally by alpha-particle emission. The alpha peak in the liquid scintillator is well separated from the ^{241}Pu β spectrum, which is comprised of low-amplitude pulses near the noise level.

If we start with pure ^{241}Pu at time $t = 0$, we can write the ^{241}Pu and ^{241}Am disintegration rates as [27]

$$\frac{dN_1}{dt} = N_1\lambda_1 = N_1^0\lambda_1 e^{-\lambda_1 t} \quad (1)$$

and

$$\frac{dN_2}{dt} = N_2\lambda_2 = (1 - f_\alpha)(N_1^0\lambda_1\lambda_2)\frac{(e^{-\lambda_1 t} - e^{-\lambda_2 t})}{(\lambda_2 - \lambda_1)}, \quad (2)$$

where N is the number of atoms, λ is the decay constant, t is the time since purification, and f_α is the ^{241}Pu alpha decay fraction. Subscript 1 denotes ^{241}Pu and subscript 2 denotes ^{241}Am.

The corresponding alpha-particle-emission rates are

$$\left(\frac{dN_1}{dt}\right)_\alpha = f_\alpha N_1^0\lambda_1 e^{-\lambda_1 t}, \quad (3)$$

$$\left(\frac{dN_2}{dt}\right)_\alpha = (1 - f_\alpha) N_1^0\lambda_1\lambda_2\frac{(e^{-\lambda_1 t} - e^{-\lambda_2 t})}{(\lambda_2 - \lambda_1)}. \quad (4)$$

* Mention of commercial products does not imply recommendation or endorsement by the National Institute of Standards and Technology, nor does it imply that the products identified are necessarily the best available for the purpose.

Adding eqs. (3) and (4) and solving for the initial ^{241}Pu disintegration rate, $N_1^0\lambda_1$, we have

$$N_1^0\lambda_1 = \frac{\left(\frac{dN_1}{dt}\right)_\alpha + \left(\frac{dN_2}{dt}\right)_\alpha}{f_\alpha e^{-\lambda_1 t} + (1-f_\alpha)\lambda_2 \frac{(e^{-\lambda_1 t} - e^{-\lambda_2 t})}{(\lambda_2 - \lambda_1)}}. \quad (5)$$

The numerator is the total alpha-particle-emission rate measured in the liquid scintillator. All of the terms in the denominator are known.

Total alpha-particle-emission-rate measurements were carried out 48 times during a period of 7.6 years using 4πα(LS)–γ coincidence, 4πα(LS)–γ anticoincidence, and 4πα(LS) integral measurements. No statistically significant difference exists between the results obtained using any of these methods.

At each measurement time, the total alpha-particle-emission rate was converted to the corresponding ^{241}Pu initial disintegration rate using eq. (5). One value was rejected and the remaining 47 values for the ^{241}Pu initial disintegration rate were fitted by linear regression. The slope of the line was less than 0.007% per year with a statistical uncertainty of slightly more than 0.007% per year (i.e., the slope is statistically indistinguishable from zero). The estimated one standard deviation of the fit at the time of purification is 0.024%.

In 1986 a dilution of this material was issued as SRM 4340 with an activity concentration of 148.4 Bq/g (July 11, 1986) with an overall uncertainty of 0.99%. The individual contributions to this uncertainty are given in table 3.

3.2. Standardization of ^{241}Pu and ^{63}Ni by 4πβ(LS) efficiency tracing with ^{3}H

The Fermi distributions for ^{3}H, ^{241}Pu and ^{63}Ni are shown in fig. 1. These were computed using the program EFFY2 [20] on the NIST CYBER 855. The Fermi distribution has the general form

$$P_i(Z, E) = C(E)F_0(Z, E)L_0(Z, E) \times (E_i - E)^2(E+1)p, \quad (6)$$

where E_i is the maximum kinetic energy of the beta particle, in units of m_0c^2, of the spectrum i, $C(E)$ is the shape factor, $F_0(Z, E)$ $L_0(Z, E)$ is the Coulombic factor, Z is the atomic number of the residual nucleus, and p is the linear momentum.

The maximum energies used for the ^{241}Pu and ^{63}Ni were those given in table 1. The ^{241}Pu and ^{63}Ni Fermi distribution maxima are shifted to lower energies, relative to tritium, primarily due to the Coulombic effect. The average energies computed for the two, 5.25 and

Table 3
Estimated uncertainties (one standard deviation or an approximation thereof) in the ^{241}Pu activity as determined from the measurement of ^{241}Am ingrowth

Source of uncertainty	Uncertainty [%]
Individual uncertainties	
(a) alpha-particle-emission-rate measurements (n = 47)	0.02
(b) gravimetric measurements	0.05
(c) dead time	0.05
(d) resolving time	0.10
(e) background	0.05
(f) pulse-height extrapolation	0.25
(g) half-lives	0.13
(h) impurities	0.10
Combined uncertainty (individual uncertainties added in quadrature)	0.33%
	× 3
Overall uncertainty (taken as three times the combined uncertainty)	0.99%

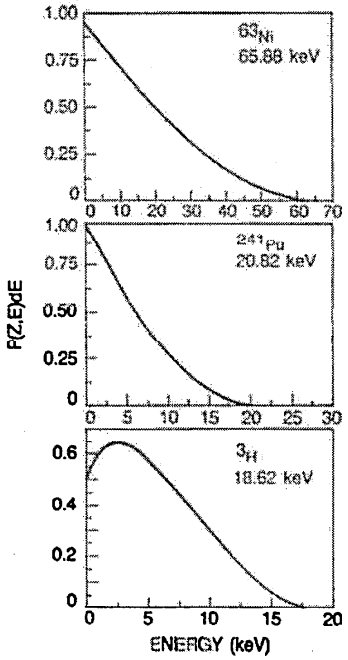

Fig. 1. Computed differential-energy spectra for three low-energy beta-particle emitters based on a Fermi distribution assuming allowed transition.

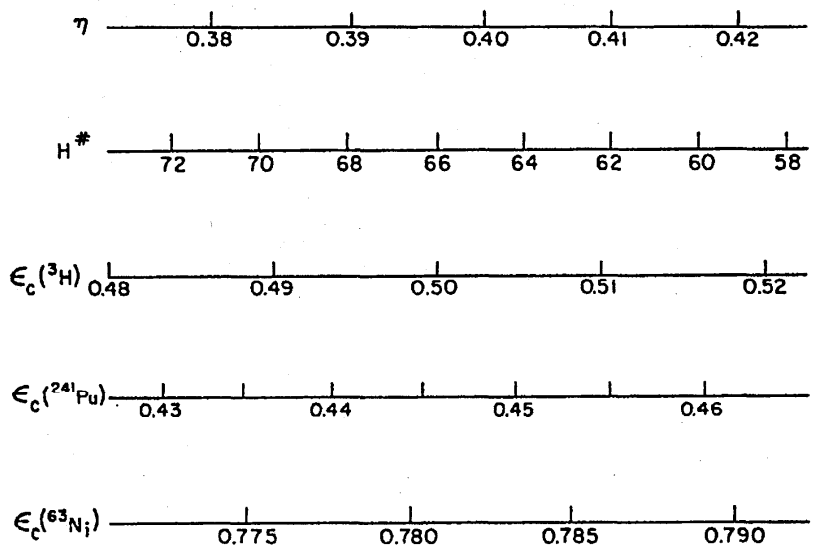

Fig. 2. Relationships between the figure of merit (η), the quench parameter ($H^{\#}$), and the two-phototube coincidence counting efficiencies for three low-energy beta-particle emitters [15]. This nomograph is strictly valid for only one scintillator and counting system.

17.16 keV, respectively, are in good agreement with those in table 1.

The efficiency tracing with ^3H involves substitution of the Fermi distribution $P(Z, E)\,dE$ for ^3H into eq. (1), and solution of the equation for the optimum value of $\eta Q(E)$. The ionization quenching function, $Q(E)$, is given by

$$Q(E) = (1/E)\int_0^E dE/(1 + kB(dE/dx)), \qquad (7)$$

where kB is the specific ionization density and dE/dx is the specific energy loss. The computed efficiencies

Table 4
Measured and computed counting efficiencies for ^{241}Pu using the Beckman model LS7800 counter and 10 ml of PCS scintillator

Sample	Horrocks' $H^{\#}$	Figure of merit, η [15]	Measured ϵ_c [a]	Computed ϵ_c [b] (eq. (1))	Difference [c] [%]
1	52.2	0.443	0.4817	0.4792	0.52
2	54.5	0.434	0.4741	0.4735	0.13
3	56.3	0.428	0.4679	0.4693	−0.30
4	60.4	0.413	0.4604	0.4590	0.30
5	61.7	0.408	0.4570	0.4560	0.22
6	67.6	0.388	0.4462	0.4421	0.92
7	71.0	0.377	0.4375	0.4337	0.87
8	72.0	0.374	0.4380	0.4312	1.55
9	72.5	0.372	0.4322	0.4300	0.51
10	73.1	0.370	0.4341	0.4286	1.27
11	75.1	0.364	0.4236	0.4240	−0.09
12	77.0	0.358	0.4236	0.4190	1.09
13	77.1	0.358	0.4198	0.4188	0.24
14	77.8	0.356	0.4222	0.4173	1.16
					Average +0.60%

[a] Measured beta-particle counting rate divided by ^{241}Pu activity from ^{241}Am ingrowth measurements.
[b] Computed using eq. (1), program EFFY2 with NIST CYBER 855.
[c] $[(\epsilon_{measured} - \epsilon_{computed})/\epsilon_{measured}] \times 100$.

Table 5
Measured and computed counting efficiencies for ^{63}Ni using the Beckman model LS7800 counter and 10 ml of PCS scintillator

Sample	Horrocks' $H^{\#}$	Figure of merit, η [15]	Measured ϵ_c [a]	Computed ϵ_c [b] (eq. (1))	Difference [c] [%]
1	57.0	0.425	0.7888	0.7932	−0.56
2	57.0	0.425	0.7864	0.7932	−0.86
3	58.8	0.418	0.7844	0.7908	−0.82
4	58.3	0.420	0.7832	0.7915	−1.06
5	58.8	0.418	0.7816	0.7908	−1.18
6	58.8	0.418	0.7848	0.7908	−0.76
7	58.9	0.418	0.7865	0.7907	−0.53
8	59.5	0.416	0.7802	0.7900	−1.26
9	60.6	0.412	0.7814	0.7885	−0.91
10	60.7	0.412	0.7827	0.7884	−0.73
11	63.4	0.402	0.7793	0.7848	−0.71
12	63.7	0.402	0.7777	0.7846	−0.89
13	64.0	0.400	0.7761	0.7840	−1.01
14	64.2	0.400	0.7799	0.7838	−0.50
15	65.8	0.394	0.7742	0.7817	−0.97
16	66.2	0.393	0.7701	0.7812	−1.44
17	67.4	0.389	0.7693	0.7795	−1.33
18	69.4	0.383	0.7743	0.7770	−0.35
19	69.8	0.381	0.7696	0.7763	−0.87
20	70.2	0.379	0.7734	0.7755	−0.27
21	70.3	0.379	0.7703	0.7755	−0.68
22	72.1	0.374	0.7671	0.7731	−0.78
23	72.1	0.374	0.7666	0.7731	−0.85
24	72.4	0.372	0.7692	0.7727	−0.46
25	73.2	0.370	0.7675	0.7716	−0.53
26	74.0	0.367	0.7649	0.7705	−0.73
				Average	−0.81%

[a] Measured beta-particle counting rate divided by ^{63}Ni activity from 1968 calorimetry measurements, using a $T_{1/2}$ value of 99.49 yr.
[b] Computed using eq. (1), program EFFY2 with NIST CYBER 855.
[c] $[(\epsilon_{measured} - \epsilon_{computed})/\epsilon_{measured}] \times 100$.

depend slightly on the value used for kB. Here we have used $kB = 0.0075$ MeV/cm based on measurements of electron-capture and isomeric-transition radionuclides which will be described elsewhere. The stopping power data, dE/dx, have been taken from Seltzer and Berger [21].

The relationships between η and the computed efficiencies for ^{3}H, ^{241}Pu and ^{63}Ni are shown in fig. 2. The efficiency for ^{3}H is measured for several samples and an empirical relationship is established between the ^{3}H efficiency and the Horrocks' $H^{\#}$. Thus, for ^{241}Pu and ^{63}Ni samples which give an $H^{\#}$ of 65, for example, the computed coincidence counting efficiencies can be taken from fig. 2 as 0.45 and 0.78, respectively. This nomograph is strictly valid for only one scintillator and counting system. The ^{3}H efficiency versus $H^{\#}$ curve must be established for each set of experimental conditions.

Tables 4 and 5 give the counting efficiency results for the ^{241}Pu and ^{63}Ni, respectively. The samples with the lowest $H^{\#}$ for each set are those which were deaerated with argon.

The principal uncertainty is that due to the ^{3}H standard source. The 0.7% uncertainty in the ^{3}H in the ^{3}H standard leads to the same 0.7% uncertainty in ^{241}Pu, but only 0.2% uncertainty in the ^{63}Ni *.

In addition to the uncertainties due to ionization quenching and those due to the ^{3}H standard solution, there are three others that should be considered because of the low energies of the β particles involved, namely, uncertainties due to:
(1) end point energies,
(2) β spectral shapes, and
(3) asymmetry of phototubes.

The first two are related. In the case of ^{63}Ni, we have followed the ENDSF evaluators [1] in assuming an

* An alternate method of efficiency tracing which is superficially similar to the one reported here has been developed by Ishikawa et al. [23], which uses ^{14}C to trace pure β emitters. Their result for a ^{63}Ni solution is 3.5% different from the certified value. As we have mentioned elsewhere [15], ^{3}H is a better choice for the tracer nuclide because it introduces less uncertainty into higher-energy radionuclides.

allowed transition of maximum energy 65.88 ± 0.02 keV. An uncertainty of 20 eV in $E_{\beta max}$ has a negligible effect on the computed efficiency.

With respect to the spectral shape, it is interesting to note that the fraction of decay events having energy greater than 5 keV for ^{63}Ni is 0.796, which is nearly equal to the coincidence counting efficiency of 0.78. The counting efficiency is strongly correlated with the low-energy fraction [22], since events for which E_β exceed 20 keV will be detected with 99% efficiency.

For ^{241}Pu, the spectral shape is not as well known. Again, we have followed ENDSF in assuming an allowed distribution and we obtain an average energy consistent with the literature [1].

Here, as in previous papers, we have assumed that the light is evenly divided between two identical phototubes. Since this is not likely to be the case, we have considered the effect of an asymmetry on the computed counting efficiencies for ^{241}Pu and ^{63}Ni. With reference to eq. (1), the argument in the exponential e^{-n_0} is the average number of photoelectrons incident on the first dynode of *one* photocathode ($n_0 = E\eta Q(E)W(E)$). By taking the square of the bracket term, we have assumed $n_1 = n_2 = n_0$. When $n_1 \neq n_2$ the bracket term in eq. (1) must be replaced by

$$[1-\exp(-n_1)][1-\exp(-n_2)]. \tag{8}$$

Assuming that the total number of photoelectrons arriving at both first dynodes is $n_1 + n_2 = 2n_0$, we introduce the half discrepancy ratio

$$\Delta n = \frac{1}{2}\frac{n_1 - n_2}{n_0}.$$

Thus,

$$n_1 - n_2 = 2n_0\,\Delta n,$$

and we obtain

$$n_1 = n_0(1+\Delta n), \quad n_2 = n_0(1-\Delta n).$$

The bracket term in eq. (1) now must be replaced by

$$[1-\exp(-n_0(1+\Delta n))][1-\exp(-n_0(1-\Delta n))]. \tag{9}$$

For a system in which $\Delta n = 10\%$, the errors introduced in the computed efficiencies for ^{241}Pu and ^{63}Ni will be 0.01% and 0.04%, respectively.

The estimated uncertainties in the ^{241}Pu and ^{63}Ni activities determined by the method of efficiency tracing with ^{3}H are given in table 6. The reference methods used to obtain the certified activity values were the 4πα(LS)–γ anticoincidence ^{241}Am ingrowth method for the ^{241}Pu, and the calorimetric method for ^{63}Ni. In order to compare the ^{63}Ni value from efficiency tracing with the earlier results, it is necessary to re-evaluate the 1968–1972 measurements in light of more recent data.

Table 6
Estimated uncertainties (one standard deviation or an approximation thereof) in the activities of ^{241}Pu and ^{63}Ni as determined by the method of 4πβ(LS) efficiency tracing with ^{3}H

Source of uncertainty	Uncertainty [%]	
	^{241}Pu	^{63}Ni
Individual uncertainties		
(a) ^{3}H gas-counting standard (0.2%)	0.20	0.06
(b) ^{3}H efficiency vs $H^\#$ calibration for scintillator (0.34%)	0.34	0.11
(c) liquid-scintillation measurements ^{241}Pu($n = 14$), ^{63}Ni($n = 26$)	0.55	0.29
(d) sample instability	0.08	0.15
(e) ionization quenching correction	0.06	0.12
(f) wall effect	nil	nil
(g) asymmetry of phototubes ($\Delta = 10\%$)	0.01	0.04
(h) uncertainty in maximum energy	0.74	0.07
Combined uncertainty (individual uncertainties added in quadrature)	1.01%	0.38%
	× 3	× 3
Overall uncertainty (taken as three times the combined uncertainty)	3.0%	1.1%

3.3. A re-evaluation of the decay data used in the calorimetric measurement of ^{63}Ni

The activity is obtained from calorimetric measurements by dividing the energy emission rate in micro-

Table 7
Summary of measurement results for NIST ^{63}Ni solution Standard Reference Material 4226D. Results corrected to December 1, 1984 using a half-life value of 100.07 (±2%) yr [2]

Laboratory	Method	Radioactivity conc. [MBq/g]	Overall [a] uncertainty [%]
NIST	calorimetry	1.347	1.1
NIST	4πβ(LS) eff. tracing with ^{3}H	1.336	1.1
AAEC [8]	eff. tracing	1.322	1.4
AECL [6]	eff. tracing	1.358	1.1
NRC [7]	eff. tracing	1.339	1.1
	mean	1.340	Std. dev. 1.1%

[a] The overall uncertainties from the earlier measurements were estimated in different ways, and they have not been re-evaluated. It is interesting to note that the standard deviation for the set of five values is in excellent agreement with the estimates of uncertainties by the different investigators.

watts by the average decay energy. Barnes et al. [2], using a maximum energy of 65.87 keV, computed an average energy of 17.23 ± 0.04 keV. A better case can be made for using the average energy from the ENDSF evaluators of 17.13 ± 0.04 keV, which changes the activity by 0.58%.

Using this value for the average energy, we have corrected the 1968 calorimetry data. The results obtained by calorimetry, and by efficiency tracing with ^{3}H, are compared in table 7 with those obtained by other investigators. It may be seen that the present results are in good agreement with the other methods.

References

[1] NCRP Report 58, A Handbook of Radioactivity Measurements Procedures, 2nd ed., ed. W.B. Mann (Washington, 1985) pp. 386, 507, (1985).

[2] I.L. Barnes, S.B. Garfinkel and W.B. Mann, Int. J. Appl. Radiat. Isot. 22 (1971) 77.

[3] G.C. Bowes and A.P. Baerg, Int. J. Appl. Radiat. Isot. 22 (1971) 431.

[4] I.W. Goodier and A. Williams, Int. J. Appl. Radiat. Isot. 22 (1971) 631.

[5] D. Smith, J.L. Makepeace and D.H. Woods, Int. J. Appl. Radiat. Isot. 38 (1987) 339.

[6] J.S. Merritt and J.G.V. Taylor, Int. J. Appl. Radiat. Isot. 22 (1971) 783.

[7] A.P. Baerg and G.C. Bowes, Int. J. Appl. Radiat. Isot. 22 (1971) 781.

[8] G.C. Lowenthal, V. Page and H.A. Wyllie, Nucl. Instr. and Meth. 112 (1973) 197.

[9] D.L. Horrocks and M.H. Studier, Anal. Chem. 33 (1961) 615.

[10] B. Denecke, A. Spernol and R. Vaninbroukx, Int. J. Appl. Radiat. Isot. 19 (1968) 812.

[11] D. Smith, in: The Application of Liquid-Scintillation Counting to Radionuclide Metrology. BIPM Monographie 3 (Sèvres, 1980) chap. 6.

[12] K. Pochwalski, R. Broda and T. Radoszewski, Appl. Radiat. Isot. 39 (1988) 165.

[13] A. Grau Malonda and E. Garcia-Toraño, Int. J. Appl. Radiat. Isot. 33 (1982) 249.

[14] B.M. Coursey, J.A.B. Gibson, M.W. Heitzman and J.C. Leak, Int. J. Appl. Radiat. Isot. 35 (1984) 1103.

[15] B.M. Coursey, W.B. Mann, A. Grau Malonda, E. Garcia-Toraño, J.M. Los Arcos, J.A.B. Gibson and D. Reher, Int. J. Appl. Radiat. Isot. 37 (1986) 403.

[16] M. Unterweger, B.M. Coursey, F.J. Schima and W.B. Mann, Int. J. Appl. Radiat. Isot. 31 (1980) 611.

[17] W.J. McDowell, in: Organic Scintillators and Scintillation Counting, eds. D.L. Horrocks and C.T. Peng (Academic Press, New York, 1971) p. 937.

[18] L.L. Lucas, ASTM STP 698, ed. J.J. Kelly (American Society for Testing and Materials, Philadelphia, PA, 1980) p. 342.

[19] Nucl. Data Sheets 44, no. (1985) 407.

[20] E. Garcia-Toraño and A. Grau Malonda, Comp. Phys. Commun. 36 (1985) 307.

[21] S. Seltzer and M.J. Berger, Int. J. Appl. Radiat. Isot. 33 (1982) 1189.

[22] B.M. Coursey, A. Grau Malonda, E. Garcia-Toraño and J.M. Los Arcos, Trans. Amer. Nucl. Soc. 50 (1985) 13.

[23] H. Ishikawa, M. Takiue and T. Aburai, Int. J. Appl. Radiat. Isot. 35 (1984) 436.

[24] P. De Bievre, M. Gallet and R. Werz, Int. J. Mass Spectrom. Ion Phys. 51 (1983) 111.

[25] D.L. Horrocks and A.L. Harkness, Phys. Rev. 125 (1962) 1619.

[26] R. Vaninbroukx, Central Bureau for Nuclear Measurements Report GE/R/RN/06/86, Geel (1986).

[27] G. Friedlander et al., Nuclear and Radiochemistry, 3rd. ed. (Wiley–Interscience, New York, 1981) chap. 5.